FORENSIC ANALYSIS OF ON-ORBIT DEBRIS GENERATION EVENTS

Marlon Sorge[1], Glenn Peterson[2], John McVey[2]

[1] *The Aerospace Corporation, 2155 Louisiana Blvd Suite 5000, NE Albuquerque, NM 87110, USA, Email*:
Marlon.E.Sorge@aero.org
[2] *The Aerospace Corporation, 2310 E. El Segundo Blvd., El Segundo, CA 90245*, USA, Email:
Glenn.E.Peterson@aero.org, John.P.Mcvey@aero.org

ABSTRACT

On-orbit fragmentation events, both collisions and explosions, continue to occur in spite of efforts to reduce their frequency through application of debris mitigation measures. Frequently the cause of these debris-producing events is not immediately known and there may be very little data available with which to determine a cause. Over the last several years The Aerospace Corporation has developed several techniques to characterize debris objects from dozens of historical fragmentation events. It has also improved its fragmentation modelling capabilities. Through these improvements it has become possible to estimate both the characteristics of the individual fragments from a debris producing event on orbit as well as the characteristics of the fragmentation event itself.

This paper will examine the approaches that have been developed to characterize the fragments and the debris-producing events. Estimates of the velocity imparted by the debris generation event (spreading velocity), fragment area-to-mass ratios and approximate mass can be made to characterize individual fragments. The results from these individual analyses can be aggregated to produce spreading speed, area-to-mass ratio (AMR), and mass distributions which can reveal key characteristics of the debris generating event, such as event time and location, and energy involved.

1 OVERVIEW

Fragmentation debris generating events have been occurring on orbit from early in the space age until the present. Fragmentation debris is distinguished from other forms of debris, such as abandoned satellites and rocket stages or debris such as lens caps, intentionally released during operations, in that it is generated from the dissociation of an object on orbit due to sudden energy releases such as explosions, or collisions with other objects, or due to material degradation such as shedding. The characteristics of debris generating events affect the properties of the resulting debris. By examining the debris from a debris producing event, it is possible to determine some of these event characteristics. These characteristics can be used to better understand the event for several purposes: anomaly resolution, modelling the amount of debris produced by the event too small to detect but which may be large enough to cause damage to satellites, and to determine the long-term effect on the orbit environment.

2 BACKGROUND

Over the course of the last several years The Aerospace Corporation (Aerospace) has characterised more than 11,000 pieces of debris from over 40 energetic fragmentation events. These events include explosions and collisions. The objects involved in the events included satellites and upper stages of a variety of types and nationalities. The likely causes of the explosion events included batteries, tank over-pressurization and residual fuel. This wide spread in event types provided a good initial set of data from which to begin relating debris and event characteristics.

Several different techniques were developed to use radar tracking information from the US Space Surveillance Network (SSN) to calculate a number of debris fragment characteristics. The characteristics examined included the spreading velocities (the velocities imparted to the fragments by the debris-producing event), the fragment AMRs, and the fragment masses.

2.1 Time-of-event and spreading velocities

The analysis method used to determine the spread velocity breakup characteristics consists of two distinct parts [1]. The first part consists of determining the time of the event while the second part determines the velocity distribution of the debris pieces (i.e., spreading velocity). To determine the best-estimate of the event time, debris objects that are identified shortly after an event are propagated backwards to find the most likely common point with the pre-event original object. In the absence of information as to the last pre-event orbit of the original object (as is often the case with newly launched upper stages that explode), the debris pieces are compared to each other to determine the time of event. The software package Collision Vision (CV) [2], which is used to support collision avoidance during launch operations, is used here to find the points of closest approach. This straightforward methodology works well when there are many debris objects identified soon after an event, but its accuracy deteriorates as the propagation time grows or if there are few debris objects that appear in the catalog

close to the event. This is an issue when examining older historical events that may have few objects that are tracked close to the event, but for which numerous objects are added at later time frames. More sophisticated optimization schemes to reduce relative errors have been developed [3], but the CV approach was used here as being more amenable to processing large numbers of events, each with large numbers of debris pieces.

The second part of the methodology was developed based on a comparison of the slowly varying orbit elements (hereafter referred to as OE) of the debris pieces and the original pre-event object. The slowly-varying elements are defined, for example, by the semi-major axis, eccentricity, inclination, right ascension of ascending node, and argument of perigee, but NOT the mean, true, or eccentric anomaly. In the case of low energy events involving near-circular orbits, the eccentricity vector can be substituted for the eccentricity and argument of perigee. Given the differences in the slowly-varying orbit elements between the pre-event primary object and the post-event debris pieces, the three spread velocity components that were imparted onto each debris piece can be estimated. The advantage of utilizing only the slowly-varying elements is that debris requiring long back propagation times to establish a connection to the breakup event can be included. This allows for additional debris objects to be added to the base data set, hopefully yielding a more accurate final spread velocity estimate.

One requirement of the OE approach is that the approximate time of the event must be known (or estimated) to be able to back propagate the slowly varying elements to their original values at the time of the event (either through SGP4 or a similar orbit element propagator; SGP4 was used in this analysis). (Examples are discussed further in Section 3.2). Therefore, the two processes (CV and OE) are used in tandem when analysing actual breakups: CV is used to determine the approximate time of the event while OE is used to develop the spread velocity distribution.

2.2   Area-to-mass ratios

Forensic analysis of the physical characteristics of debris is accomplished by an orbit determination process that estimates the ballistic coefficient over an interval of time, the fit span. The most abundant source of orbital data for debris are two-line element (TLE) sets. The TLE data are treated as observables in the estimation process to determine the ballistic coefficient over that fit span for a given epoch. The process is repeated over all available TLE sets for each piece of debris, providing a collection of ballistic coefficients from which other metrics can be derived [4]. For forensic analysis, it is necessary to use only the area-to-mass ratio portion of the ballistic coefficient. Recall that the ballistic coefficient is the drag coefficient multiplied by the area-to-mass ratio. To estimate the area-to-mass ratio, the drag coefficient is

computed within each orbit determination solution. Analysis of these area-to-mass ratio estimates leads to a wealth of information about each debris, such as mass given radar cross-section (RCS) measurements, material density approximation, long-term attitude trends, and shape approximation in some cases [5]. Recent debris producing events from NOAA-16, Sentinel-1A, and WorldView-2 satellites will each serve as examples to illustrate the application of the ballistic coefficient estimation technique. This technique can yield valuable insight into the characteristics of the individual debris objects, collision and explosion events and their associated parent objects. The result of this improved knowledge of debris characteristics will translate into improved fragmentation modelling, orbit lifetime estimates, collision risk analyses, and the mitigation of future growth to the debris environment.

2.3   Masses

Mass is one of the fundamental properties of debris fragments. An estimate of the masses of the debris from a breakup event can provide insight into how complete the fragmentation event was, where complete fragmentation means that the entire object was fragmented versus only a small fraction of the object(s). Mass is also an important parameter in determining the amount of energy involved in the fragmentation event, particularly in an explosion where there is not necessarily any kinematic information to assist in the energy determination process.

Fragment mass estimation is based on the estimation of area-to-mass ratio discussed in section 2.2. Given a sufficient amount of state information in the observations over a long enough time period, which is dependent on the altitude of the debris orbit, a fairly accurate estimate of the average area-to-mass ratio can be made for each piece of debris. In order to extract an estimate of the fragment mass, an estimate of the fragment's cross-sectional area is required. This estimate is currently taken from the average radar cross-section measurements from the SSN. Generally the longer the time period over which the RCS measurements were taken the better the estimate. The extended time period produces more measurements with potentially different geometric perspectives on the debris to average out orientation and rotational axis-induced biases as well as to include multiple radar sites. Consideration also needs to be taken for the potential differences due to radar site wavelength particularly for debris that are sufficiently small to be on the order of the wavelength of the radar.

The use of RCS for deriving an approximate area has a number of potential problems that can affect the area estimates. RCS can be affected by the shape of an object as well as its material composition. Because both of these are likely unknown for debris fragments there can be significant uncertainties in the resulting mass estimates

as compared to the determination of area-to-mass ratio and spreading velocity. In order to make an estimate of the potential variability caused by the sometimes indirect relationship between physical area and RCS, the debris from a number of historical fragmentation events were analysed and an estimate of the total mass of the observed fragments was made [6]. Since the original mass of the object was known, a comparison could be made between the known mass and the estimated total mass of the fragments. The errors for typical complete fragmentations, where "typical" means objects composed primarily of metals, were generally 40% or less with about half being less than 20%. The errors tended to be equally likely to be positive or negative. Some cases with more difficult materials, such as one with a composite over-wrapped tank, had higher errors. In that case the errors were closer to 60% which is to be expected given the complications that the composite material may cause in terms of its RCS to physical size relationship.

One of the most common sources of error in the total mass estimates was found to be attributable to certain fragments that consistently showed a much higher RCS value than was likely possible. These fragments, based on their typically small area-to-mass ratios, would then produce very large mass estimates. The objects could frequently be identified by comparing the mass estimate and the spreading speed estimates. These objects tended to show up as significant outliers with unrealistic imparted kinetic energies.

The general accuracy levels, although not as high as would be preferred, are sufficient to discern important information about fragmentation events including whether the event was a complete or partial fragmentation. They are also sufficient to generate distributions of cumulative number versus mass since the debris is being examined in aggregate, and so for events with a large number of fragments the trend of the distribution can be established.

3 EVENT CHARACTERISTIC DETERMINATION

Three events were selected as representative sample cases. A large amount of debris was released from the NOAA-16 satellite in late 2015 and was chosen as representative of a large debris producing event. The Sentinel-1A event was included to provide an example of what is widely considered to be a collision involving an impact on the solar array. The third event involved the WorldView-2 satellite. WorldView-2 was included since it may have had a similar cause to Sentinel-1A and can allow a comparison of the debris from potentially similar events. The three satellites (NOAA-16, Sentinel-1A, and WorldView-2) were all in near Sun-synchronous inclinations but at different altitudes (850 km, 700 km, and 765 km respectively).

3.1 Time of event/location determination

The NOAA-16 satellite was observed to have a debris-generating event on November 25, 2015 (day-of-year 329), which produced almost 400 pieces of debris of trackable size (i.e., >10 cm) and an unknown amount of debris too small to be tracked. The main satellite experienced a small change in the semi-major axis of approximately 16 meters (Figure 1), but the other orbit elements (to the level of accuracy of the two-line element sets) showed no noticeable change.
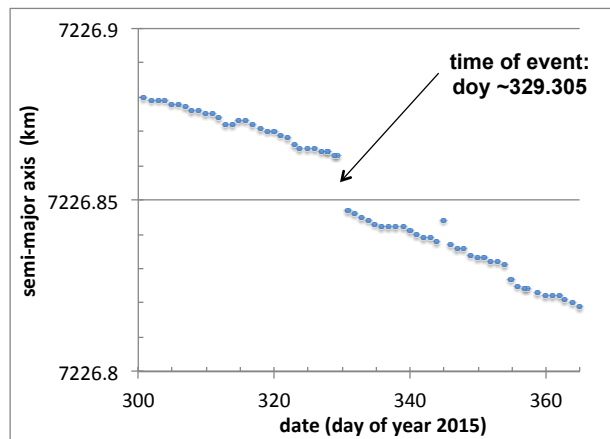
Figure 1. NOAA-16 semi-major axis time history

One of the issues that arises from examining large debris events is how quickly the individual debris pieces can be uniquely determined and catalogued. Figure 2 exhibits the problem and shows the number of debris pieces associated with NOAA-16 as they appeared in the public Resident Space Object catalog. The initial group of catalogued debris was identified within 10 days of the event and consisted of 53 objects. These were the objects used in determining the time of event. However, "new" objects were being identified and placed into the catalog as late as 247 days after the event. This delay in attribution is a product of both the difficulty in both observing small debris-sized objects and, as the time of event recedes into the past, attributing those objects to their originating event.
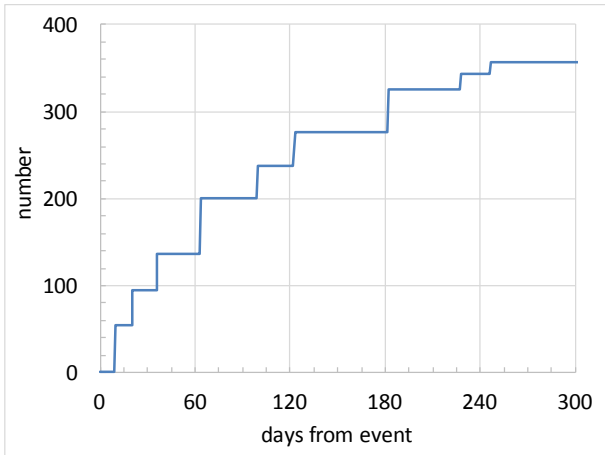
Figure 2. NOAA-16 debris as it appeared in the public catalog

The actual time of event was found through comparison of the initial group 1 debris TLE sets to the last pre-event TLE of the main satellite (the "initial debris" included the first post-event TLE of the main satellite as well). Figure 3 shows the results of the close approach times for the resulting conjunctions placed into 1 minute bins. Only conjunctions that yielded a miss distance of less than 10 km were retained. Under these conditions, the average time of the event was found to be 07:18:34 UT with a standard deviation of 228 seconds. Geographically, this time would correspond to when the main satellite was on an ascending pass just past Antarctica.
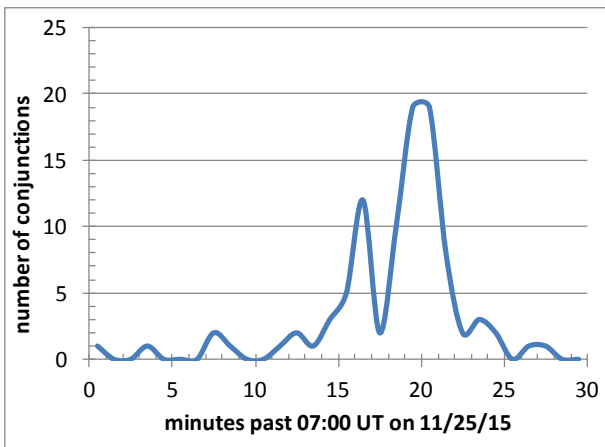
Figure 3. NOAA-16 estimated time of event

As another example of the time/event determination, consider the Sentinel-1A event which occurred on August 23, 2016. Seven pieces were identified and tracked within days of the event. However, the main satellite showed no change in its orbital elements (to within the accuracy of the two-line element sets) which implies that the satellite did not experience a significant change in momentum. Propagating backwards in time to find a common point of intersection resulted in a time of event of 17:06:46 UT, but given the few number of debris

pieces, the standard deviation on the Sentinel-1A time was larger than it was for NOAA-16 at 1630 seconds. As with NOAA-16, geographically, Sentinel-1A was over Antarctica when the event occurred.

WorldView-2 gave off nine pieces of debris on July 18, 2016. Computing the time of event from the debris yielded an estimated time of conjunction of 22:59:22 UT with a standard deviation of 415 seconds. Geographically, WorldView-2 was over the North Pole at the time of event. Part of the reason for the better solution of WorldView-2 when compared to Sentinel-1A (even though both had few debris pieces) lies in the relatively rapid appearance of the WorldView-2 debris in the catalog as opposed to the Sentinel-1A debris (~1 day vs. 7 to 10-day gap). Another factor was that Sentinel-1A was at a lower, and hence more drag influenced, altitude than WorldView-2 (700 vs 760 km), which introduced more uncertainty into the propagation.

3.2 Spreading velocity distributions

Histograms for the NOAA-16 spreading velocity estimate are shown in Figure 4-Figure 6. The benefit of utilizing the slowly varying orbit element method can now be observed. Due to the growth of along-track uncertainties, only the initial group of tracked debris could be included in the solution for the event time. However, by basing the spreading velocity solution on the slowly varying elements, all 357 pieces of debris could be included. The resulting average magnitude of the spreading velocity that was imparted to the debris pieces was ~30.8 m/sec with the distribution shown in Figure 4. Most of the debris experienced velocities on the order of <50 m/sec, but a small portion had larger velocities of up to 144 m/sec. Figure 5 shows a histogram of the spreading velocity angles of the debris pieces in the local horizontal plane (0 degrees = along-track direction; 90 degrees = orbit normal direction). The green dots indicate what a perfectly spherical distribution would look like on this plot. The imparted spread velocities are fairly distributed over 360 degrees. Figure 6 shows a histogram of the spreading velocity angles of the debris pieces in the local vertical plane (-90 degrees = down towards the Earth direction) with again the green dots indicating what a spherical distribution would appear to be. Combining these histograms implies that the debris spread out uniformly in the horizontal plane with little debris pushed up or down. The lack of a dominant spike or lobe in the distribution histograms might be indicative of an explosive event as opposed to a collision, which would tend to have a noticeable spike or lop-sidedness.
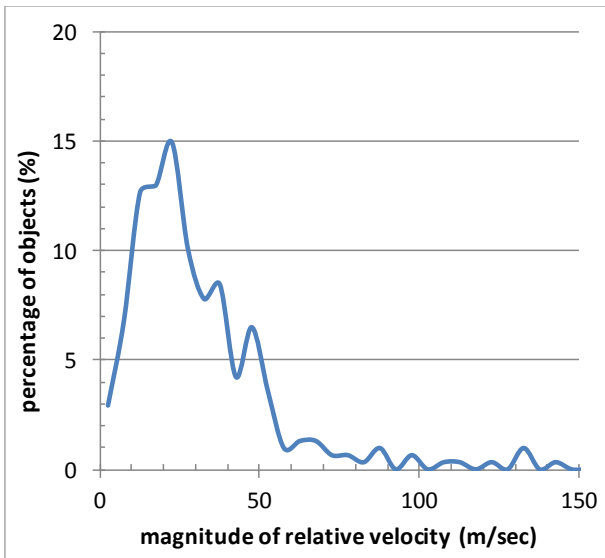
Figure 4. NOAA-16 histogram of spreading velocity magnitudes
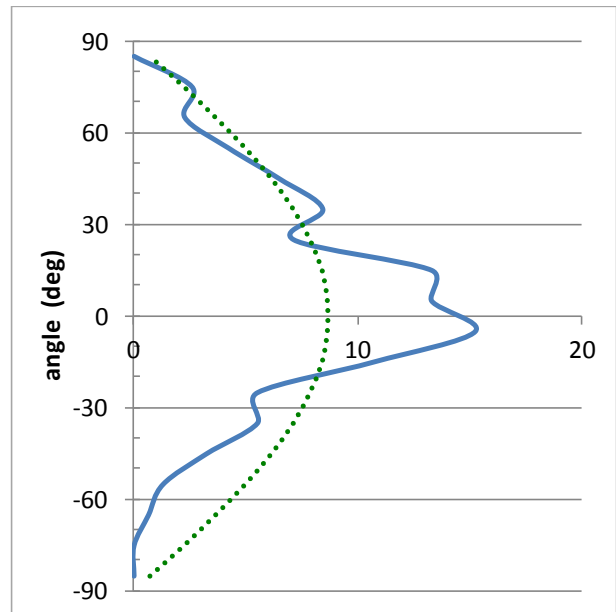
Figure 6. NOAA-16 histogram of local vertical angles of spreading velocities

For Sentinel-1A, the debris experienced an average velocity change of approximately 13.6 m/sec in magnitude while the main satellite exhibited virtually no change in its velocity. With fewer pieces, full histogram plots proved problematic and instead the individual components of the spreading velocity solution are shown in Figure 7 with R being in the radial direction (outward from the Earth), T is along-track, and N denotes the orbit normal direction. The spread velocity distribution was dominated by pieces (5 of the 7) that were pushed to the left, upwards, and towards the direction of motion, suggesting that an impacting object likely came from the right. However, there were also two pieces pushed to the left as the other pieces were but towards the backwards direction. These characteristics (majority of the debris being pushed into a single general direction without a "blowback" of debris in the opposite direction) could indicate that the Sentinel-1A debris was composed of materially thin components of the spacecraft, for example, the solar arrays or external antennas.

Figure 5. NOAA-16 histogram of local horizontal angles of spreading velocities
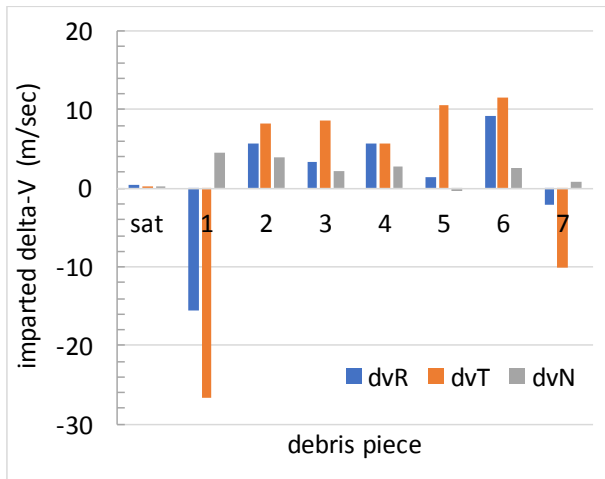
Figure 7. Sentinel-1A spreading velocity solution results

WorldView-2 debris pieces showed a spreading velocity average magnitude of 9.95 m/sec. Figure 8 shows the spread velocity component results. As with Sentinel-1A, the main satellite experienced little to no change in its velocity. For the debris, four pieces were pushed to the left, upwards, and into the velocity vector direction while one piece (#4) showed large anti-along-track and anti-orbit normal components and two other pieces, 6 and 8, experiencing large spreading velocities along the anti-orbit normal direction. In other words, pieces 1, 2, 5, and 7 were pushed in a direction roughly opposite to pieces 4, 6, and 8. This distribution dominated by a single directionality with significant opposite component ("blowback") would be more indicative of a collision rather than an explosion.
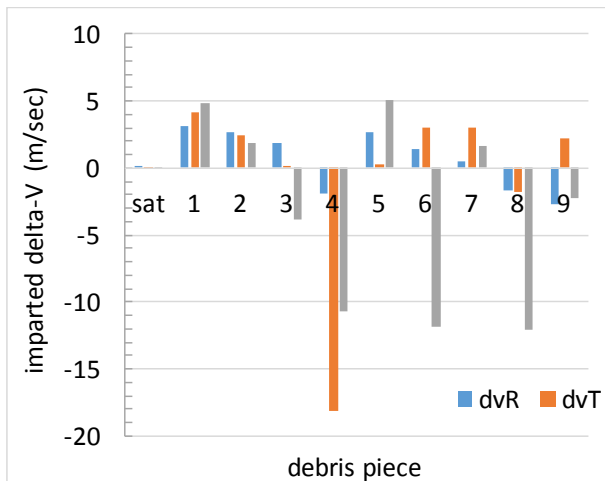
Figure 8. WorldView-2 spreading velocity solution results

3.3 Area-to-Mass Ratios

Debris fragment area-to-mass ratios provide some insight into material properties of the debris including rough density information. The area-to-mass ratio estimation

process also provides insights into the quality of the estimations. The debris events, such as NOAA-16, is a different type of breakup event from Sentinel-1A, and WorldView-2, and yield different information about debris-producing events. The parent objects consist of many different materials, which are dispersed amongst the debris during these breakups. The debris from these events will be a subset of these materials, but could contain multiple materials in one object. Therefore, the density of the debris will be difficult to determine uniquely, but will generally fall into three categories, high, medium, and low density material. Evaluating the weighted average of all the estimated area-to-mass ratios for a given piece of debris is key to approximating their material density individually. The weighting formulation assigns higher weights to the area-to-mass ratios with lower residual values from their orbit estimations and visa-versa. The debris from NOAA-16, Sentinel-1A, and Worldview-2 were analysed, and the area-to-mass ratio estimates were determined. Figure 9 depicts the time series of these estimates for one piece of Sentinel-1A debris along with their corresponding average root sum square (RSS) residual values for each fit. These estimates typically oscillate within a range due to non-sphericity of the debris, noise and errors within the data and the estimation process itself. However, through the experience of analysing many vehicle breakups, there exists a range of area-to-mass ratio estimate values that corresponds to material densities for fragmentation events. Low values of area-to-mass ratio estimates (0.001 – 0.1 m^2/kg) tend to be denser materials like steel, titanium, and some aluminium alloys toward the higher end of this range. High values of area-to-mass ratio estimates (1 - 10 m^2/kg) tend to be lower density materials like multi-layer insulation (MLI), carbon composites, and solar panel fragments. Estimated values in the middle range of estimated values (0.1 - 1 m^2/kg) are more difficult to determine due to the approximate nature of this technique. Typically the debris fragments could consist of most aluminium alloys, and electronic components like circuit board material. The following breakup examples demonstrate how to use the area-to-mass ratio estimates to infer what materials comprised the released debris. Knowledge of the materials provides more context about the breakup event.
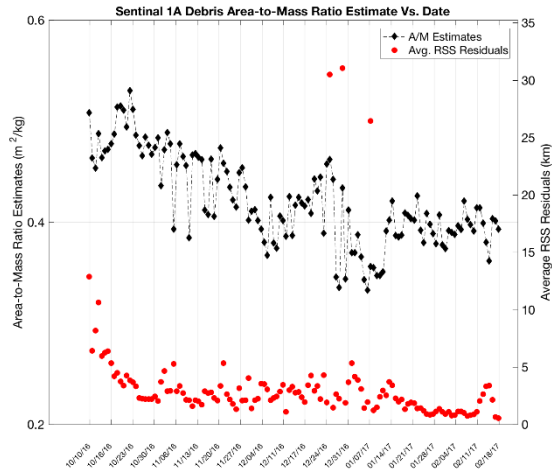
Figure 9. Debris pieces from Sentinel-1A AMR estimates
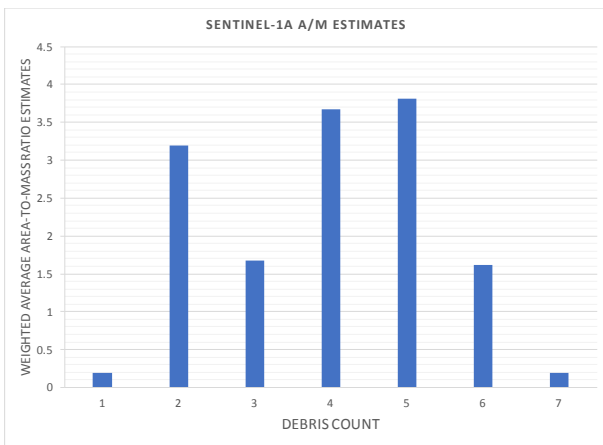
Figure 10. Sentinel-1A AMR Estimates

Figure 10 shows the weighted average area-to-mass ratio estimates for the debris released from the Sentinel-1A collision event. The estimated values for five of the debris pieces fall into a range between 1 - 4 m^2/kg, which suggests lighter materials like carbon composite, insulation, or solar panel fragments. The other two pieces of debris are in the medium density range and suggest materials like an aluminium, or circuit board/solid electronics at estimated values around 0.1 – 0.2 m^2/kg. When comparing Figure 7 (Sentinel 1A spreading velocity to Figure 10 (area-to-mass ratio estimate), it is interesting to note that the two debris pieces that experienced out-of-family spread velocity solutions also exhibited very different area-to-mass ratio estimates.
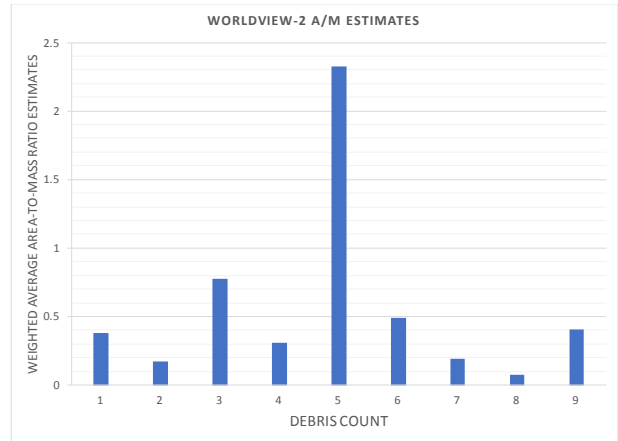
Figure 11. WorldView-2 AMR Estimates

Figure 11 depicts the weighted average area-to-mass ratio estimates for the debris released from the WorldView-2 collision event. Many estimated area-to-mass ratio values for the debris correspond to medium density materials which may represent aluminium or solid electronic fragments with one lighter piece of debris (~2.3 m^2/kg) representing composite or MLI.
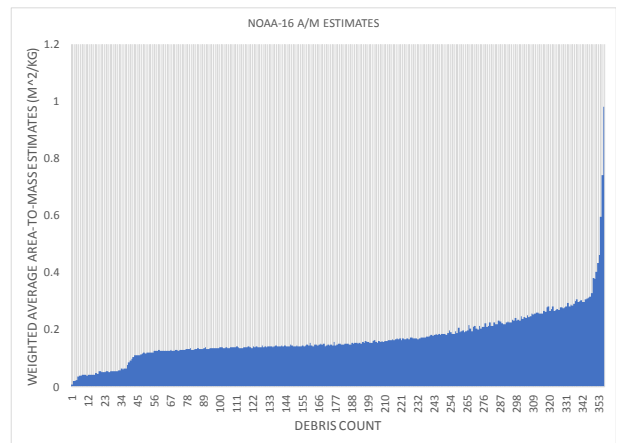
Figure 12. Weighted average AMR estimates for all NOAA-16 debris

Figure 12 shows the weighted average area-to-mass ratio estimates for the debris released from the NOAA-16 event. There are hundreds of debris fragments released that span all the material ranges. There are ~40 estimated values in the lowest range indicating higher density materials like steel or more solid blocks of less dense materials. The remainder of debris fall into the medium density range possibly representing aluminium, or solid electronics. There were only a few potentially low density materials as part of the total debris count.

3.4   Debris Physical Characteristics

Information on the physical characteristics of debris objects can be derived from considering both individually and jointly several of the parameters that have been discussed previously including the area-to-mass ratio and mass. This information can provide indications of the types of materials of which the debris may be composed and can be used to infer possible sources for that debris.

The analysis of NOAA-16 debris discussed in previous sections suggests that the total mass of the debris generated by the event was approximately 36 kg. That is approximately 2% of the total satellite dry mass. This can be compared to the fragmentation events such as the Delta 2 upper stage explosions from the 1980's which produced a similar number, or fewer, of trackable debris fragments and yet involved the whole vehicle. This demonstrates that the number of trackable fragments from a debris-producing event is often a poor indicator of the characteristics of the fragmentation event itself.

The Sentinel-1A and WorldView-2 events both appear to have similar causes. Analysis of the debris from these events shows that the total mass of debris in each case is less than 1 kg. It should be noted that this is more than an order of magnitude less than the mass of the NOAA-16 debris. This set of data, in the absence of any other, would be sufficient to suggest that the NOAA-16 event was significantly different than the Sentinel-1A and WorldView-2 events.

In the case of Sentinel-1A the debris mass was estimated as 0.1-0.2 kg. In the case of the WorldView-2 debris the total debris mass is closer to 0.8 kg. It should be noted that because of the uncertainties in the RCS-size relationship these mass values could be expected to have similar uncertainties as were discussed earlier. Given the uncertainties the total debris masses are similar between the events.

To examine a specific example of combining debris characteristics consider the NOAA-16 debris. Figure 13 shows a plot of the area-to-mass ratio versus mass for over 350 pieces of debris from the NOAA-16 event. Also plotted on the figure are a section of the debris from the 2007 fragmentation of the Chinese FengYun-1C (FY-1C) satellite. The two events both involved satellites as the fragmenting objects but differed in that the FY-1C event was a collision which involved several orders of magnitude more energy than the NOAA-16 event, which was likely not a collision. Because of the much higher energies involved in the FY-1C event the entire satellite was fragmented as could be determined by a fragment mass determination analysis as was discussed in Section 2.3. The NOAA-16 debris includes only a small fraction of the total satellite mass.

Whereas the debris from FY-1C represents an entire satellite, the debris from NOAA-16 is only 2% of the mass. The area-to-mass ratio versus mass plot shows that the NOAA-16 debris represents a subset of the possible range of debris from a satellite. It can be seen that the debris from NOAA-16 tends to occupy a similar range of area-to-mass ratios to that of the main concentration of FY-1C debris in the range of masses from 0.01 − 0.05 kg. Although, with the much smaller amount of mass represented by the NOAA-16 debris, it would not be expected that the extreme ranges of the area-to-mass ratio would be fully populated, it is notable that there are essentially no NOAA-16 debris with area-to-mass ratios above 1, the range where one might expect MLI and other insulation, particularly noticeable in the masses below 0.01 kg. Why this is so is not clear. It may be that the potion of the satellite involved in the event did not have large amounts of MLI or that any pieces generated were too small to track. The larger NOAA-16 debris (> 0.05 kg) tend to be in the upper portion of the range of area-to-mass ratio values seen in the FY-1C debris. Particularly in the mass range above 0.1 kg there are NOAA-16 fragments in the higher, less populated area-to-mass ratio ranges, which differs from the behaviour at smaller masses. These higher area-to-mass ratio fragments are less likely to be MLI and insulation than the smaller fragments which may explain the population of the highest area-to-mass ratios at the higher masses, but not in the lower mass ranges.
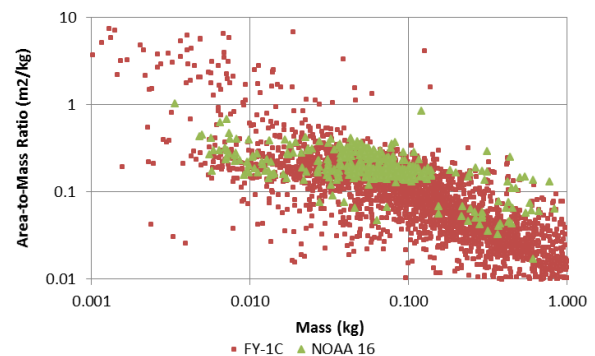
Figure 13. NOAA-16 and FY-1C AMR versus mass comparison

A plot of area-to-mass ratio versus mass for the Sentinel-1A and WorldView-2 debris is shown in Figure 14. The two sets of debris cover a similar range of area-to-mass ratio and are largely near the top of the range of area-to-mass ratio values at a given mass when compared to the FY-1C debris in Figure 13. This suggests that the debris is primarily composed of less dense materials. It is important to make the comparisons of area-to-mass ratio as a function of mass (or size) as area-to-mass ratios will increase proportional to the inverse of the cube root of mass (or like the fragment radius) due solely to geometric considerations when excluding material and shape variations.
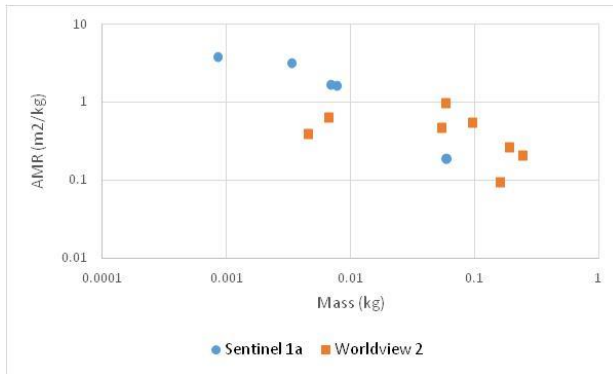
Figure 14. Sentinel-1A and WorldView-2 AMR vs mass comparison

The interpretation of debris characterization data is still in an early stage of development. It is expected that the significantly more detailed fragment characterization data from the DebriSat test [7] will assist in improving the interpretation of the debris characterization information.

3.5   Event energy determination

One of the important parameters in understanding a fragmentation event is the amount of energy that was used to drive the fragmentation. This information, particularly for explosions and other single initial object events, is needed not only to help determine or substantiate a proposed cause, but also to model the event in order to determine the risk of its trackable and untrackable debris to operational satellites.

In order to provide near-real-time risk assessments for satellites after a breakup event or to provide timely inputs for investigations into debris producing event causes, it is necessary to be able to derive the fragmentation energy from information or approximations that are available shortly after the event occurs. The most quickly observable parameter that is most directly related to breakup energy is the spreading speed. An approach was developed to estimate the fragmentation event energy which is discussed in [8]. The approach uses the average spreading speed of SSN observed fragments or radar tracks along with a total mass of fragments. The mass can be the total mass of the object for catastrophic breakups, and an estimate, usually based on historical information, for non-catastrophic events.

This technique has been extended to lower energy events since the publication of [8] in order to incorporate information from a number of sub-catastrophic breakups, both collisions and explosions.

To estimate the event energy, a relationship was derived between the average spreading speed of the observed fragments, the mass of the object, and its physical type (satellite or upper stage) and the total energy of the fragmentation event. For sub-catastrophic events, where

the majority of the parent objects remains in a single piece, it is also necessary to determine the mass of the fragments, excluding the main body, which must be used in place of the object mass. When attempting to estimate energy before there is sufficient time and tracking information to determine debris object area-to-mass ratios and therefore mass, estimates of the fragment mass must be used based on similar historical events. These early energy estimates can be updated as sufficient data becomes available so that the techniques described in the previous sections can be used.

4   IMPACTS BY SUB-TRACKABLE DEBRIS

4.1   Overview

Based on models of the existing debris environment it would be expected to see impacts on satellites and upper stages from debris that is too small for the SSN to track. Most of the objects in orbit are inactive and it is possible that the impacts of small fragments might not be noticed as they would produce little trackable debris which could be the only observable indication that a collision had occurred. In the case of operational satellites small impacts should produce momentum or orbit energy changes that would be detectable by on-board sensors. Additionally the greater tracking resources expended on tracking active satellites might increase the probability that even small amounts of debris could be detected.

Over the last few years several debris-producing events have occurred that suggest impacts by sub-trackable debris objects. These events have typically involved the generation of few pieces of debris trackable by the SSN, typically less than a dozen. The fragments tend to display fairly low spreading speeds and have very low masses indicating that the events involved relatively little energy.

4.2   Example cases

Several likely sub-trackable debris impacts have occurred over the last few years. Two of the more recent events involving Sentinel-1A and WorldView-2 have been discussed in previous sections. One of the earlier events was the creation of a piece of debris from the BLITS satellite on January, 2013. BLITS was a laser ranging satellite that contained no internal energy sources to power a fragmentation. A study performed by The Aerospace Corporation suggested that the event was due to the impact of a small, few millimetre-sized fragment [3] based on the characteristics of the debris, a single additional piece that is trackable with a spreading speed on the order of 1 m/s.

Another example of a likely collision with a sub-trackable piece of debris is the debris producing event involving the Iridium 91 satellite which occurred on November 30, 2014. The event resulted in 4 pieces of

debris tracked by the SSN. Analysis of these fragments using the techniques described previously determined that the total fragment mass was less than one kilogram and that the spreading speeds were between 10 and 100 m/s. The total kinetic energy represented by the spreading debris was estimated to be on the order of 100 J. Based on the modelled estimates of total energy delivered the information suggests that an object of 1-3 mm impacted the satellite. This estimate is based on assumptions of most probable material and closing speed for the debris.

These likely small object collision events tend to share some common characteristics. One of the commonalities of these events mentioned previously is that the spreading velocity distributions tend to favour certain directions versus being relatively uniform as was seen with the NOAA-16 debris. Often the majority of the debris will have been accelerated in a particular direction. The debris from these events also tend to have very low total imparted kinetic energies. The estimated energies for the Iridium 91, Sentinel-1A, and WorldView-2 debris were in the range of 10's to 100 J. These are orders of magnitude lower than observed explosion events. The low imparted kinetic energies are a function of the typically low total fragment mass and low spreading speeds observed with these events. Finally it is interesting to note that a large fraction of these events, where an event time could be determined, occurred near the earth's poles. This is the region where a number of highly inclined orbits, including those for the objects in the two major debris producing events of the last decade, FY-1C and the collision of the Cosmos 2251 and Iridium 33 satellites, cross each other. The locations of the small object collisions is where it would be expected to be most probable, but there are still too few events to draw definitive conclusions.

5 SUMMARY/CONCLUSIONS

During the last several years Aerospace has been developing a number of tools for determining the characteristics of debris fragments from more than 40 on-orbit fragmentation events. The techniques have been applied to a wide range of objects, event types, and event energies including both collisions and explosions. Examination of these debris events demonstrated that the debris has different characteristics distinctive to the events that created them. Aerospace's continued analysis has begun correlating the debris characteristics to specific properties of the events including completeness of fragmentation and the energy involved in the event. This field is still in the early stages of development and Aerospace continues work to advance and refine the analysis techniques and interpretation of data. It is expected that data from ground tests as well as additional on-orbit data will enable significant improvements to the interpretation of fragmentation debris forensic analysis.

6 REFERENCES

1. Peterson, G. E., (2013). Use of Slowly Varying Orbit Elements for Spread Velocity Reconstruction of Historical Orbital Breakups. *AAS/AIAA Astrodynamics Specialist Conference*, AAS 13-845.

2. Gist, R. G., and D. L. Oltrogge, Collision Vision: Covariance Modeling and Intersection Detection for Spacecraft Situational Awareness, Paper No. AAS 99-351, AAS/AIAA Astrodynamics Specialist Conference, Girdwood, Alaska, July, 1999

3. Thompson, R., Peterson, G.E., McVey J.P., Markin, R.E., Sorge, M.E. (2013). BLITS: A Forensic Analysis of a Probable Collision. *AAS/AIAA Astrodynamics Specialist Conference*, AAS Paper 13-907, AAS.

4. McVey, J. P. (2011). Automated Ballistic Coefficient Estimation Technique to Analyze the Debris from the COSMOS-2251 and IRIDIUM-33 Collision. *AAS/AIAA Astrodynamics Specialist Conference*, AAS 11-412.

5. McVey, J.P. (2016). Characterization of Space Debris from the Cosmos-2251 and Iridium-33 Collision Event Using Ballistic Coefficient Estimation. Ph.D. thesis, University of Southern California.

6. Sorge, M. E., Mains, D. L., (2016). IMPACT Fragmentation Model Developments. *Acta Astronautica.* **126**, 40-46.

7. Rivero, M., Shiotani, B., Carrasquilla, M., Fitz-Coy, N., Liou, J.-C., Sorge, M., Huynh, T., Opiela, J., Krisko, P., Cowardin, H. (2016). DebriSat Fragment Characterization System and Processing Status. 67th International Astronautical Congress. IAC-16.6.2.8x35593.

8. Hoots, F. R., Sorge, M.E. (2012). Satellite Breakup Parameter Determination. *Journal of Astronautical Sciences.* **59**(1&2), 123-143.